Supplementary information

Catalytic consequences of Ga promotion on Cu for CO₂ hydrogenation to methanol

Juan C. Medina[a], Manuel Figueroa[a], Raydel Manrique[a], Jhonatan Rodríguez Pereira[b,c], Priya D. Srinivasan[d], Juan José Bravo-Suárez[d], Víctor G. Baldovino Medrano[b,c], Romel Jiménez[a], Alejandro Karelovic[a]*

* Corresponding author: akarelov@udec.cl

[a] Laboratorio de Carbono y Catálisis (CarboCat), Departamento de Ingeniería Química, Facultad de Ingeniería, Universidad de Concepción, Concepción, Chile.

[b] Centro de Investigaciones en Catálisis (@CICAT-UIS), Parque Tecnológico Guatiguará (PTG), Km. 2 vía El Refugio, Universidad Industrial de Santander, Piedecuesta (Santander), 681011, Colombia.

[c] Laboratorio de Ciencia de Superficies (#SurfLab-UIS), Parque Tecnológico Guatiguará (PTG), Km. 2 vía El Refugio, Universidad Industrial de Santander, Piedecuesta (Santander), 681011, Colombia.

[d] Chemical & Petroleum Engineering Department, The University of Kansas, Lawrence, Kansas 66045, USA

S1 Mass and heat transfer limitations

In order to obtain meaningful reaction rates, these have to be measured in the absence of mass transport limitations or temperature gradients. There exist experimental and theoretical methods to study the magnitude of the transport processes in fixed bed reactors to verify if the reaction rates are effectively kinetically controlled. In this work equations proposed by Vannice[1] were used for this purpose.

S1.1 Intraparticle temperature gradients

In the case of heat transfer, the verification of the following equation permits to conclude that the intraparticle temperature gradients are insignificant:

$$\frac{|\Delta H|\, r\, R_p^2}{\lambda\, T_S} < \frac{0.75\, T_S\, R}{E_t}$$

(S5-1)

Where $|\Delta H|$ is the absolute enthalpy of reaction, r corresponds to the measured rate of reaction, R_p is the radius of the catalyst particles, λ stands for the thermal conductivity of the support material, T_S is the temperature on the external part of the particles, R is the gas constant and E_t the apparent activation energy.

Data used corresponds to RWGS at 280°C for the most active catalysts in mass normalized rate of reaction (CuGa1/SiO$_2$), and using the most pessimistic values of the variables.

$|\Delta H|$ = 49.5 kJ/mol

r = 0.66 µmol/g/s = 0.91 mol/m³/s (SiO2 bulk density = 2500 kg/m³, bed porosity assumed = 0.448)

R_p = 75 µm

λ = 1.3 W/K/m

T_S = 280°C

R = 8.314 J/mol/K

E_t = 131 kJ/mol

Using equation S5-1 it is observed that the inequality is largely satisfied:

$2.9 \times 10^{-7} < 2.6 \times 10^{-2}$

Consequently, the temperature gradients in the catalysts particles are assumed to be negligible.

S1.2. Intraparticle concentration gradients

For intraparticle mass transfer the Weisz-Prater dimensionless number is calculated. It relates the rate of reaction to that of diffusion in the particle pores. If the Weisz-Prater number is lower than or equal to 0.3 the internal diffusional limitations can be considered negligible:

$$\frac{r\ R_p^2}{C_S\ D_{eff}} \leq 0.3$$

(S5-2)

Besides the terms already defined, here C_S is the concentration of reactant on the catalyst surface and D_{eff} is the effective diffusion coefficient. For the experiments of this work the values are:

r = 0.91 mol/m³/s

R_p = 75 µm

C_S = 44.1 mol/m³

D_{eff} = 8.57×10^{-6} m²/s

In this case the criterion is largely satisfied since Weisz-Prater number is 1.93×10^{-12}

S1.3 Interphase concentration gradients

In the case of gradients between the bulk gas phase and the surface of catalyst particles, an effectiveness factor has been defined (ψ) which relates the measured rate of reaction with the reaction rate without diffusional limitations. The product of the effectiveness factor with the Dahmköhler number (Da_0) which relates the rate of reaction with the rate of transport from the bulk of the fluid to the catalyst surface is composed of observable magnitudes:

$$\psi Da_0 = \frac{r}{k_g \, a \, C_0}$$

(S5-3)

Where k_g is the mass transfer coefficient between the fluid and the surface of catalyst particles, a is the ratio area/volume of catalyst particles and C_0 the concentration of reactant in the bulk of the fluid.

Data for the system studied here are the following:

r = 0.91 mol/m³/s

k_g = 0.04 m/s

a = 22100 m²/m³

C_0 = 44.1 mol/m³

Consequently, the product ψ Da_0 equals 2.5×10^{-5}, and ψ is approximately 1, which means that external mass transfer artifacts are negligible.

Taking into account the above results one can safely assume that the reaction took place in fully kinetic regime.

S2. XPS spectra

In this section the XPS spectra and their decomposition are shown for a representative catalyst (CuGa2/SiO$_2$). The spectra for the other catalysts were qualitatively the same and are not shown for the sake of brevity. Spectra for C1s, O1s and Si1s show a surface charge effect evidenced by the broadening of the peaks at lower binding energy. However, this does not affect the quantification of the different elements. Additionally, as Cu and Ga did not suffer from this effect, their binding energies and oxidation state assignments are not affected.
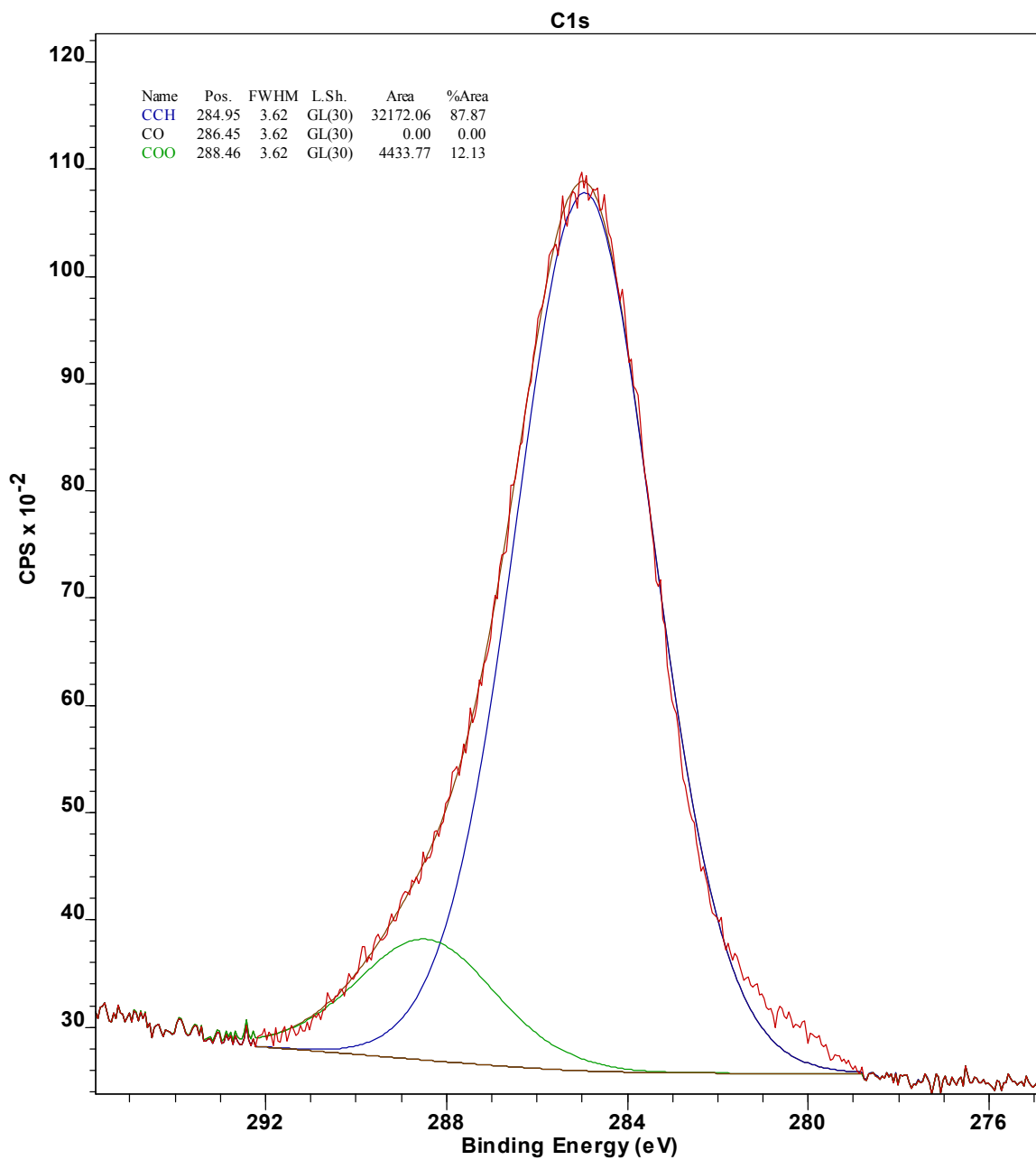
Figure S1: XPS spectrum of C1s region for CuGa2/SiO$_2$ catalyst.
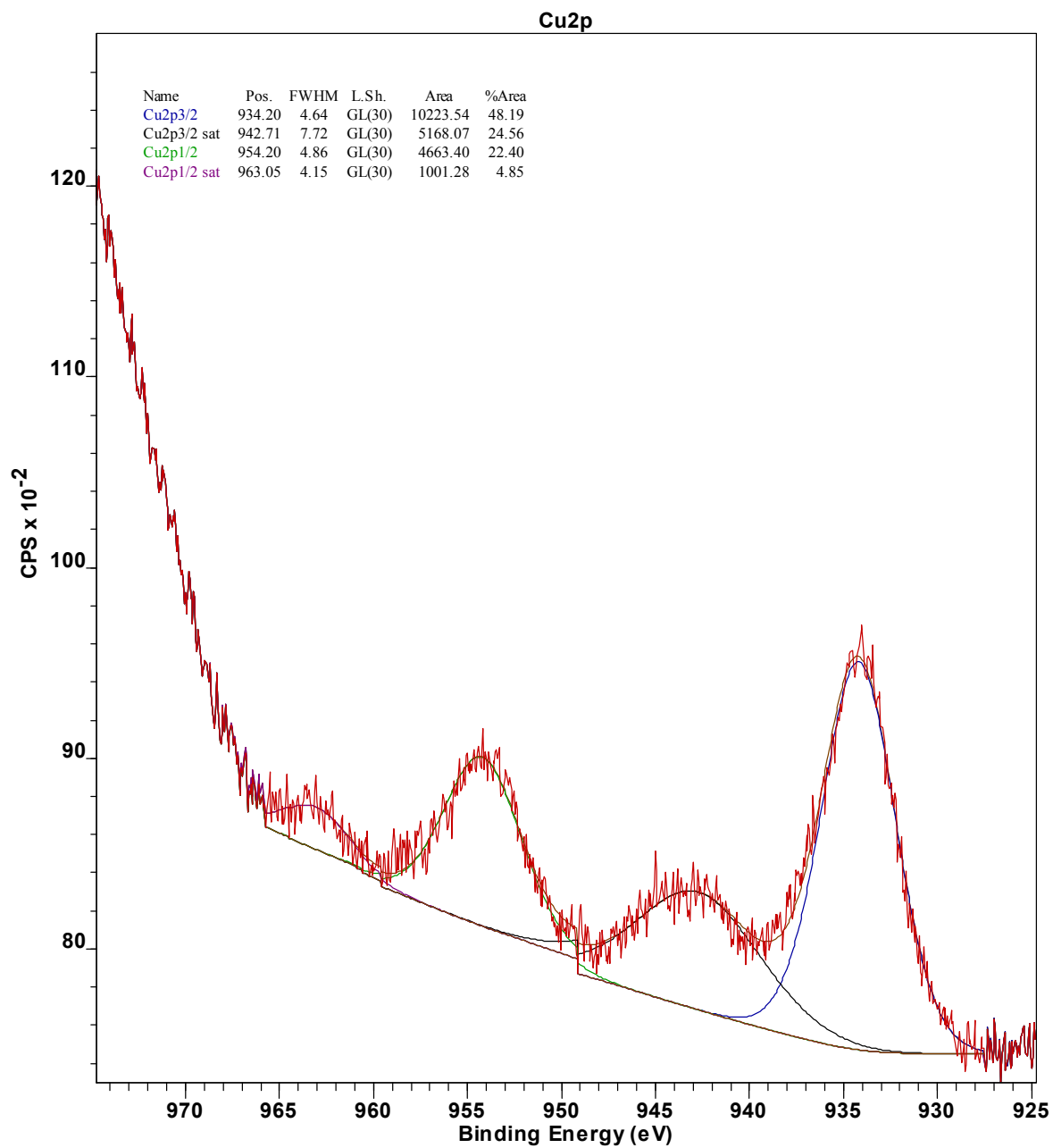
Figure S2: XPS spectrum of Cu2p region for CuGa2/SiO$_2$ catalyst.
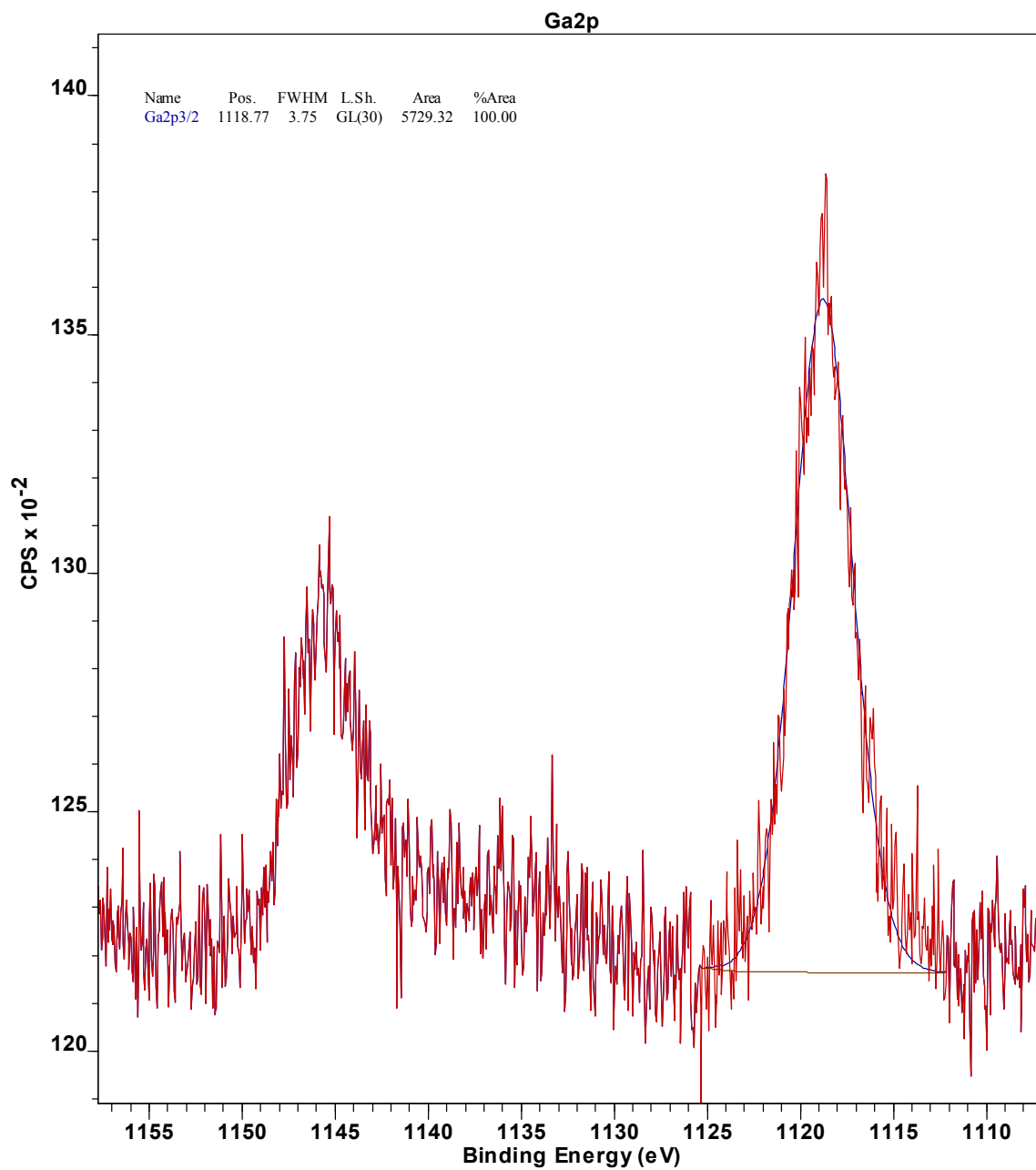
Figure S3: XPS spectrum of Ga2p region for CuGa2/SiO$_2$ catalyst. Ga2p$_{3/2}$ peak (appearing at 1118.78 eV) was used for Ga quantification.

O1s

Name	Pos.	FWHM	L.Sh.	Area	%Area
O1s	532.67	3.30	GL(30)	108597.81	91.54
O1s	529.67	3.30	GL(30)	10060.31	8.46

CPS x 10^{-3}

Binding Energy (eV)
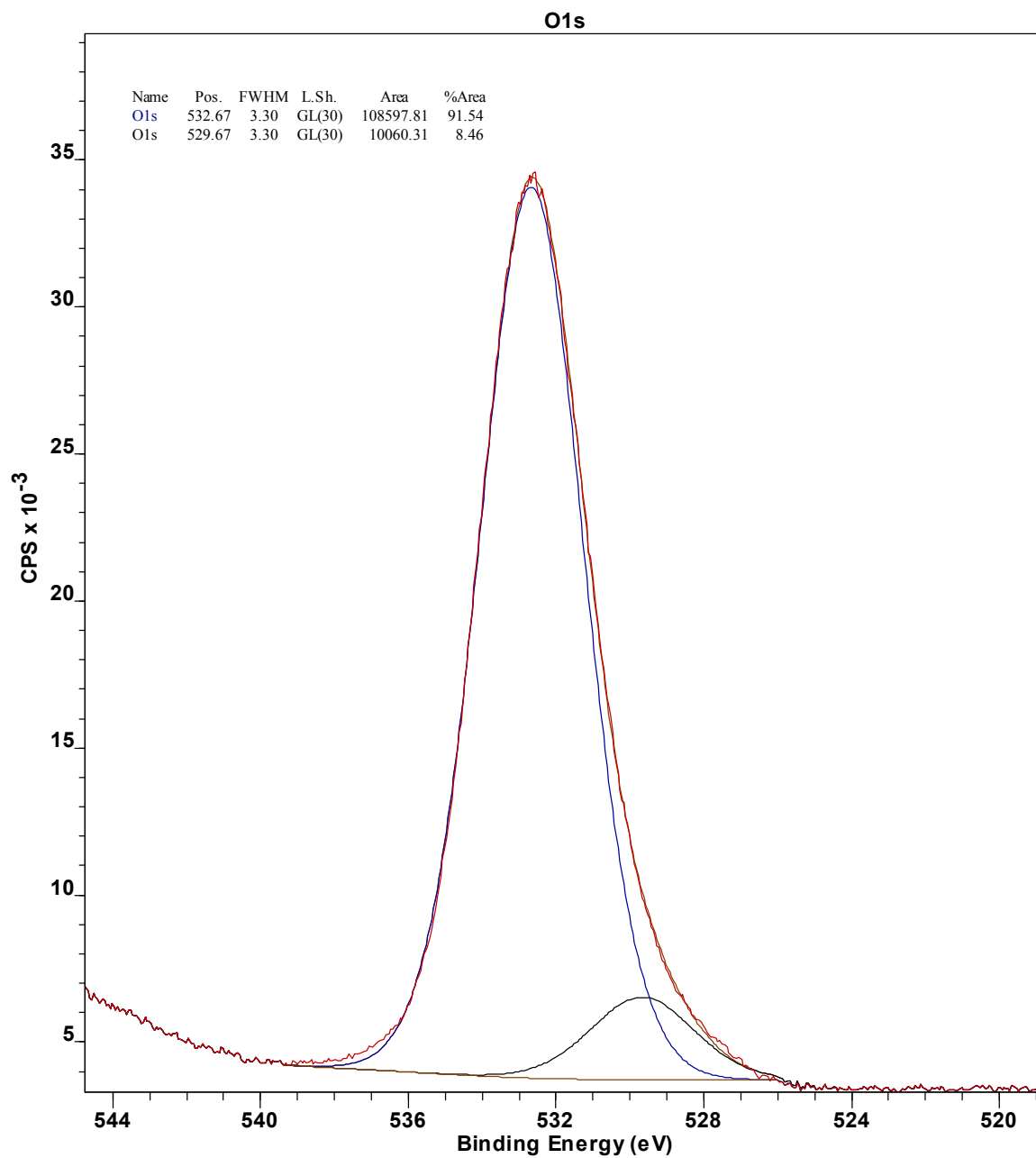
Figure S4: XPS spectrum of O1s region for CuGa2/SiO$_2$ catalyst.
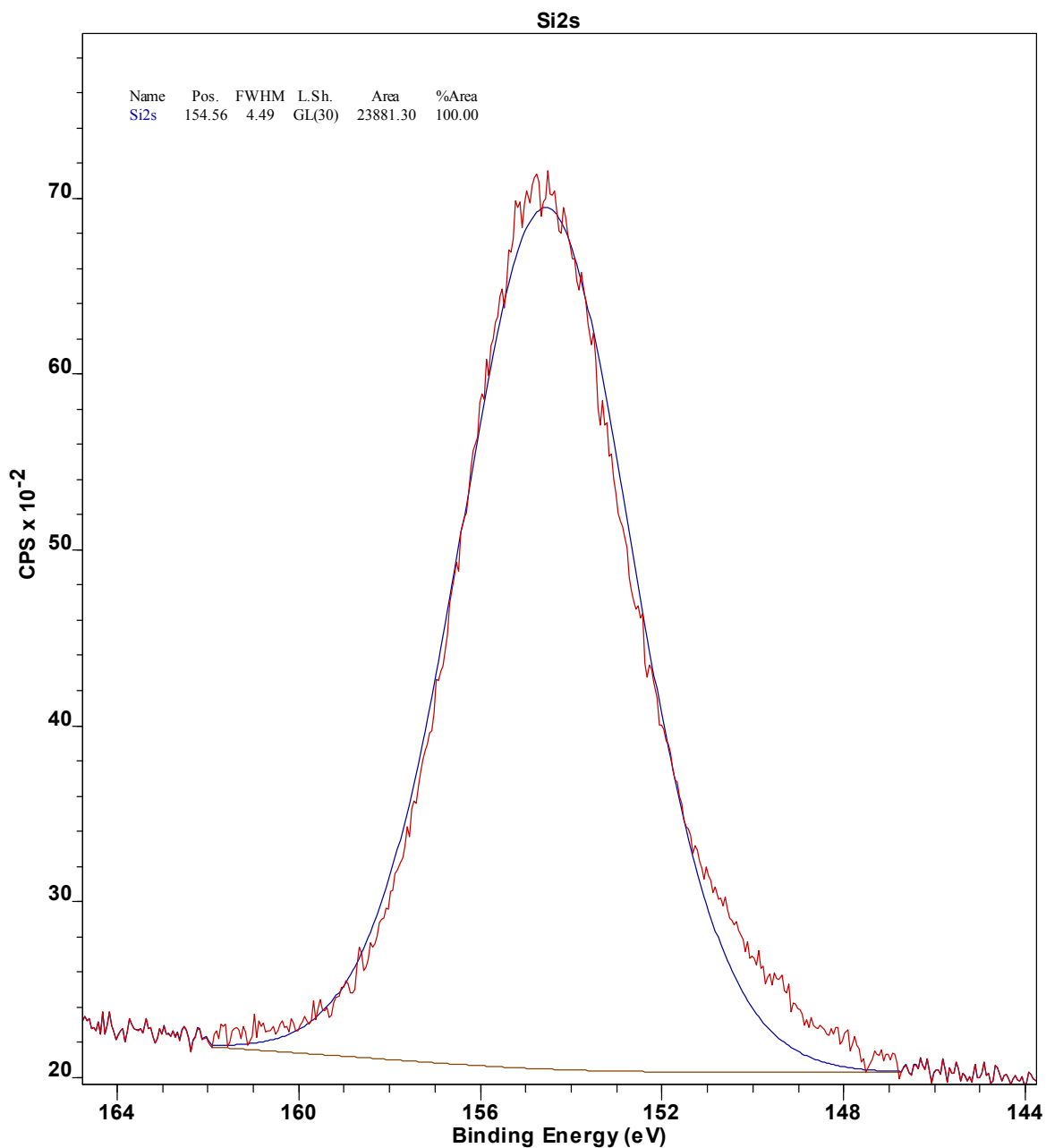
Figure S5: XPS spectrum of Si2s region for CuGa2/SiO$_2$ catalyst.

S3. Derivation of methanol synthesis rate equations using Langmuir-Hinshelwood assumptions

S3.1 <u>Formate hydrogenation (step 1.4) is the RDS</u>.

We take all the steps before the RDS as being in equilibrium:

$$\theta_H = \sqrt{K_1 P_{H2}} \theta_* \quad \text{(S3-1)}$$

$$\theta_{CO2} = K_2 P_{CO2} \theta_* \qquad \text{(S3-2)}$$

$$\theta_{HCOO} = \frac{K_3 \theta_{CO2} \theta_H}{\theta_*} \qquad \text{(S3-3)}$$

The rate of methanol formation is the rate of step 1.4:

$$r_{MeOH} = k_4 \theta_{HCOO} \theta_H \qquad \text{(S3-4)}$$

Replacing Eq. S3-1 to S3-3 into S3-4 one obtains the reaction rate in terms of observables:

$$r_{MeOH} = k_4 K_1 K_2 K_3 P_{CO2} P_{H2} \theta_*^2 \qquad \text{(S3-5)}$$

S3.2 Formic acid hydrogenation (step 1.5) is the RDS

In this case, Eq. 1-4 is assumed to be in equilibrium, which gives the following equation:

$$\theta_{HCOOH} = \frac{K_4 \theta_{HCOO} \theta_H}{\theta_*} \qquad \text{(S3-6)}$$

The RDS defines the rate of methanol formation:

$$r_{MeOH} = k_5 \theta_{HCOOH} \theta_H \qquad \text{(S3-7)}$$

Consequently, if one replaces Eq. S3-6 into Eq. S3-7 and utilizes Eqs. S3-1 through S3-3, one arrives to the following equation:

$$r_{MeOH} = k_5 K_1^{3/2} K_2 K_3 K_4 P_{CO2} P_{H2}^{3/2} \theta_*^2 \qquad \text{(S3-8)}$$

S3.3 Methoxy hydrogenation (step 1.8) is the RDS

The RDS defines the rate of methanol formation:

$$r_{MeOH} = k_8 \theta_{H3CO} \theta_H \qquad \text{(S3-9)}$$

Steps prior the RDS could be considered at equilibrium. We can thus write the following equations:

$$\theta_{H2COOH} = \frac{K_5 \theta_{HCOOH} \theta_H}{\theta_*} \qquad \text{(S3-10)}$$

$$\theta_{H2CO} = \frac{K_6 \theta_{H2COOH} \theta_*}{\theta_{OH}} \qquad \text{(S3-11)}$$

$$\theta_{H3CO} = \frac{K_7\theta_{H2CO}\theta_H}{\theta_*}$$ (S3-12)

We can combine these three equations to obtain:

$$\theta_{H3CO} = \frac{K_5K_6K_7\theta_{HCOOH}\theta_H^2}{\theta_{OH}\theta_*}$$ (S3-13)

Additionally, at steady state the rate of methanol production (S3-9) should be equal to the rate of water production (1-10). Consequently, we can write the following relation:

$$r_8 = r_{10}$$ (S3-14)

$$k_8\theta_{H3CO}\theta_H = k_{10}\theta_{OH}\theta_H$$ (S3-15)

We can combine equations S3-13 and S3-15, and use the additional equilibrium relations (S3-1 to S3-3 and S3-6) to obtain:

$$\theta_{H3CO}^2 = \frac{k_{10}}{k_8}K_1^2K_2K_3K_4K_5K_6K_7P_{CO2}P_{H2}^2\theta_*^2$$ (S3-16)

This equation is introduced in S3-9 to obtain:

$$r_{MeOH} = K_1^{1.5}\sqrt{k_8k_{10}K_2K_3K_4K_5K_6K_7}P_{CO2}^{0.5}P_{H2}^{1.5}\theta_*^2$$ (S3-17)

S4. Derivation of RWGS rate equations using Langmuir-Hinshelwood assumptions

The RDS is assumed to be the dissociation of CO2 (step 2.3). Consequently:

$$r_{CO} = k_3\theta_{CO2}\theta_*$$ (S4-1)

Step 2.2 can be considered at equilibrium:

$$\theta_{CO2} = K_2P_{CO2}\theta_*$$ (S4-2)

This gives the following reaction rate equation for RWGS:

$$r_{CO} = k_3K_2P_{CO2}\theta_*^2$$ (S4-3)

We assume that adsorbed CO is the most abundant surface intermediates, and that free sites are significant.

$$1 = \theta_* + \theta_{CO}$$ (S4-4)

If we assume that step 2.4 can be considered at equilibrium, we can write:

$$\theta_{CO} = K_4 P_{CO}\theta .$$
(S4-5)

Combining equations S4-3 to S4-5, the RWGS rate equation has the following form:

$$r_{CO} = \frac{k_3 K_2 P_{CO2}}{(1 + K_4 P_{CO})^2}$$
(S4-6)

S5. Fitting of RWGS model to experimental data

We used and **integral reactor approach** and used a minimization of least squares to fit the equation S4-6 to the data presented in 5a and 5b for CO formation. The average deviation is 6% for Cu/SiO_2 data and 8% for $CuGa5/SiO_2$ (See Figure S6). Clearly, more data, and at different temperatures are needed to validate the model. However, this model qualitatively describes and explains why the apparent reaction order of RWGS reaction with respect to CO_2 experimentally lies between 0.3 and 0.5 instead of 1, which is the prediction based on the generally assumed CO_2 dissociation step as RDS.
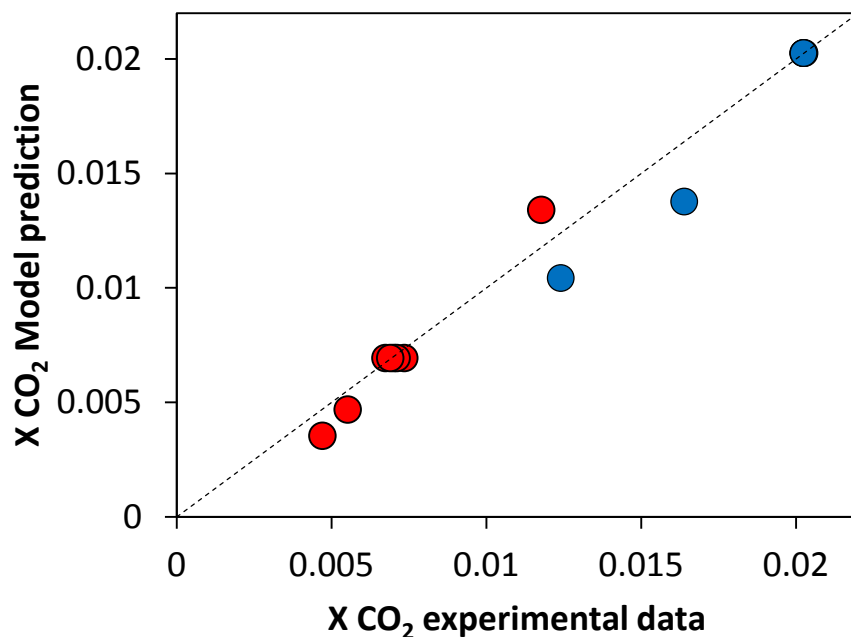
Figure S6. Parity plot for RWGS model of equation S4-6. CO_2 conversion predicted by the model compared to experimentally measured CO_2 conversion. Red circles: $CuGa5/SiO_2$ catalysts. Blue circles: Cu/SiO_2 catalyst. T = 260 °C. P = 800 kPa.

S6. Kinetic data.

Table S1: Conversion (X), selectivity (S) and turnover frequencies (TOF) obtained for experiments at different temperatures.

Catalyst	T (°C)	S CO (%)	S CH_3OH (%)	X CO_2 (%)	CH_3OH TOF (s^{-1})	CO TOF (s^{-1})
Cu/SiO$_2$	280	95.2	4.8	3.5	4.22E-05	8.18E-04
	270	94.3	5.7	2.2	3.15E-05	5.16E-04
	260	93.5	6.5	1.4	2.27E-05	3.24E-04
	240	91.0	9.0	0.5	1.09E-05	1.10E-04
CuGa1/SiO$_2$	240	60.9	39.1	0.5	1.62E-04	2.51E-04
	260	80.2	19.8	1.4	2.53E-04	1.00E-03
	280	88.9	11.1	3.0	3.16E-04	2.33E-03
CuGa2/SiO$_2$	240	40.7	59.3	0.6	2.86E-04	1.95E-04
	260	65.0	35.0	1.0	3.11E-04	5.66E-04
	280	78.0	22.0	2.1	4.45E-04	1.44E-03
CuGa5/SiO$_2$	240	48.1	51.9	0.5	2.96E-04	2.73E-04
	260	68.4	31.6	1.0	3.90E-04	8.30E-04
	280	82.3	17.7	2.1	4.89E-04	2.12E-03
CuGa10/SiO$_2$	240	68.7	31.3	0.4	1.42E-04	3.11E-04
	260	80.6	19.4	1.0	2.10E-04	8.63E-04
	280	89.0	11.0	1.9	2.40E-04	1.89E-03

References

1 M. A. Vannice, *Kinetics of Catalytic Reactions*, Springer US, Boston, MA, 2005.